Water Dispersible Semiconductor Nanorod Assemblies via a Facile Phase Transfer and Their Application as Fluorescent Biomarkers

Ambarish Sanyal,[a] Tanushree Bala,[a] Shafaat Ahmed,[a] Ajay Singh,[b, a] Anna V. Piterina,[c] Timothy M. McGloughlin,[c] Fathima R. Laffir[a] and Kevin M. Ryan[a, b*]

Abstract

We demonstrate the formation of water dispersed nanorod assemblies by phase transfer of semiconductor (CdS, CdSe, CdTe) nanorods from the organic to the aqueous using pluronic triblock copolymers. On phase transfer, the randomly dispersed nanorods in the organic medium close pack in the form of discs encapsulated in the hydrophobic core of water dispersible micelles. The assemblies showed excellent cellular uptake exhibiting membrane and cell specific fluorescence at low light intensity under confocal microscopy.

Notes and references

Introduction

Close packed semiconductor nanorod assemblies where each one dimensional nanocrystal adopts a side by side ordering and uniform axial orientation are a significant recent discovery. While discrete nanorods show polarized light emission, length dependent photon absorption and high fluorescence cross-sections, [1, 2] their collective assembly can allow scaleable applications in next generation LED's, photovoltaics and field emission devices. [3-10] Nanorods have been directed into perpendicularly ordered assemblies either by using external electric fields or by evaporation control at solid/liquid or liquid/air interfaces.[11-14] The aspect ratio and polydispersity of the rods in addition to solvent-evaporation dynamics plays a key role in achieving vertical alignment and close packing from solution. In effect, the gradual packing of randomly dispersed nanorods into a reducing solvent volume allows attractive dipole-dipole and Van der Walls forces between ligand capped nanorods to dominate the assembly behaviour at a substrate. [15] Assemblies of nanorods dispersed in solution is also interesting in particular where individual properties such as linearly polarised emission can be collectively harnessed for example as novel fluorescent biomarkers. [16, 17] In non polar solvents, ligand capped nanorods are randomly dispersed in dilute solutions but can form nematic liquid crystals (LC) phases in more concentrated dispersions. [18] The LC behaviour is dynamic and is destroyed outside of local temperature and concentration variations limiting discrete application. More robust and potentially biocompatible nanorod assemblies can be achieved when nanorods are stabilised in the aqueous phase as micelles. Nie *et al*. functionalised gold nanorods with hydrophilic CTAB ligands grafted along the rod sides with hydrophobic polystyrene on the rod ends which assembled into either discrete chains or spherical bundles depending on the water concentration in mixed DMF or THF solvents. [19] More recently Zhuang *et al*. achieved water dispersible disc shaped CdS/ CdSe nanorod assemblies in a two stage process by further co-ordinating individual alkyl capped nanorods with a dual interaction ligand (dithiol-functionalised Tween-20, Tween-SH) followed by annealing in ethylene glycol at 80 ^{o}C. [20]

In this report, we demonstrate a facile single-step, room temperature route to the formation of water dispersible nanorod assemblies of CdS, CdSe and CdTe using triblock copolymer surfactants of the form $PEO_xPPO_yPEO_x$ (PEO: polyethylene oxide, PPO: polypropylene oxide). These types of copolymers are known to self-assemble to form morphological variations of spherical, vesicular or mesophasic aggregates in aqueous solutions and are widely used in the pharmaceutical industry to solubilise hydrophobic drugs. [21, 22] Here, we discovered that the facile stirring of an organic solution of alkyl capped nanorods mixed with an aqueous solution of the triblock copolymer resulted in the formation of very stable aligned nanorod assemblies in the aqueous phase. The phase transfer occurs whereby discrete alkyl capped nanorods in the organic phase are transferred to the aqueous phase via encapsulation in hydrophobic polypropylene oxide core of a triblock micelle. The resultant close packed disk shaped assemblies consists of rods tethered only by the interdigitation of the original long chain alkyl ligands suggesting the triblock copolymer does not co-ordinate to each individual nanorod but to the rod ensemble. *In vitro* analysis showed an excellent uptake of the water dispersed nanorod assemblies by human vascular smooth muscle cell and the occurrence of various spectral properties via this interaction (membranous and intracellular) demonstrate their potential as fluorescent labels.

Experimental

Materials

Cadmium oxide (>99%) was purchased from Fluka, Trioctylphosphine (TOP, 90%), trioctylphosphine oxide (TOPO, 99%), sulfur (99.98%), selenium (99.98%) and telerium (99.98%) were purchased from Aldrich. n-octadecylphosphonic acid (ODPA), n-tetradecylphosphonic acid (TDPA), *n*-hexylphosphonic acid (HPA), *n*-octylphosphonic acid (OPA) was obtained from PolyCarbon Industries Inc (PCI). The block-coploymers F88, F127, P123, P65 were obtained from BASF Germany. All the chemicals were used as received. Filter paper of pore sizes 2.5 micron and 0.45 micron were purchased from Whatman and Milipore Corporation respectively for size selective separation of the nanorods assemblies through filtration.

Synthesis of CdS nanorods

The CdS nanorods utilised in this study were synthesised essentially through the pyrolysis method, [23] redispersed in toluene and kept under N_2 environment inside a glove-box. In a typical experiment 800 μL of sulphur-tri-octylphosphine mixture was injected to a hot mixture of cadmium oxide and surfactants ODPA and TOPO (1: 2:>4 by molar ratio) at a temperature of 300 ^{O}C. The reaction was quenched after 30 mins by adding a suitable quantity of toluene. Stoichiometric amount of acetone was added to precipitate the nanorods (average length and diameter around 25-30 nm and 6-8 nm respectively), following which they were centrifuged and redispersed in toluene. A drop of CdS nanorods solution was then deposited and allowed to evaporate onto carbon-coated Cu grids for transmission electron microscopy (TEM) characterization. Evaporation of the resulting solution led to the formation of a 2D array of CdS superlattice with the rods aligned in a perpendicular direction.

Synthesis of CdSe nanorods

CdSe nanorods were synthesised with slight modifications to the published procedure. [4] The general approach for the synthesis of nanorods involves the stepwise addition of cadmium precursor and followed by chalcogenide precursor at a high temperature. Briefly, CdO (0.2 g) as a cadmium precursor was dissolved in mixture of surfactants like n-tetradecylphosphonic acid (TDPA, 0.71 g), *n*-hexylphosphonic acid (HPA, 0.160 g) and tri-n-octylphosphine oxide (TOPO, 3.00 g) in 25 ml three-neck flask equipped with a condenser and a thermocouple adapter. The mixture was heated to 120º C in an atmosphere of Ar and then degassed for 60 min with pressure range between 150 – 300 mTorr and followed by heating at 300ºC under Ar atmosphere, during which the CdO decomposed and gave an optically clear solution. Once clear solution was achieved 1.5g of trioctylphosphine (TOP) was added to the mixture and the temperature was further raised to 310ºC. Next stock solution of Selenium (~500μl) containing 0.073 g of selenium in 0.416 g of TOP was injected rapidly to the vigorously stirring precursors and the resulting particles were further allowed to grow for 5-10 min at 310ºC.The nanorods

growth was terminated by removal of the heating mantle, and at 80ºC 2-4 ml anhydrous toluene was added to the mixture to quench the reaction. The nanorods were purified by dissolution in toluene and precipitation from anhydrous isoproponal. They were cleaned thrice with toluene and isoproponal mixture and redispersed in toluene for further measurements.

Synthesis of CdTe nanorods/ dipods/ tetrapods

CdTe was also synthesised in a procedure exactly similar to that of CdSe. Unlike in the case for CdSe, ODPA (0.812 g), TOPO (2.65 g), OPA (0.315 g) was used along with CdO. The tellurium stock solution (~ 500 µl) containing 0.061g of tellurium in 0.552 g TOP was rapidly injected (less than 1.0 s) to the vigorously stirring Cd solution and particles were allowed to grow for 4 minute at 310 ^{o} C. It eventually turned out that concentration of CdTe tetrapods and dipods were more than the nanorods in the resultant product. They were then cleaned thrice with toluene and methanol mixture and redispersed in toluene for further measurements.

Phase transfer of CdS, CdSe and CdTe nanorods/ tetrapods

5ml of 3% of the block copolymers (Pluronic F88, F127, P123, and P65, obtained from BASF Germany) was mixed with 5ml of the diluted CdS nanorods in toluene and was allowed to stir intensively for 12 hrs until there was a clear observation of an appearance of colour in the aqueous phase (see photographs of Fig. 1). The top organic layer was carefully separated and later discarded. The remaining aqueous layer was centrifuged and washed a couple of times with deionised water in order to remove excess unbound surfactants. Aliquots from these resulting solutions were taken and used for further characterizations. Phase transfer was accomplished with 5% and 20% F88 in the same manner. In order to have an idea of the flexibility of the process, CdSe nanorods and CdTe dipods/ tetrapods dispersed in toluene were also phase transferred with 3% F127 and treated in a similar manner before characterization.

Cell Culture and Cellular uptake of CdS nanorods

 Vascular Smooth Muscle Cells (VSMC) (PromoCell, Germany) were grown in monolayers at 37°C in a humidified atmosphere at 5%CO_2 in 5% Fetal Bovine Serum – VSMC media supplemented with penicillin/streptomycin. At 85 % confluence, cells were detached from a 75 cm^2 flask surface by treatment with 0.25% trypsin and a 0.02% EDTA in Ca $^{2+}$ and Mg $^{2+}$ free PBS (pH 7.3). Cells were plated for 24 h before the experiment on poly-L-lysine-coated glass cover slips at 5 × 10^3 cell/cm^2. After incubation for 12 hours with CdS nanorods /VSMC media at 37^{0}C in a humidified 5% CO_2 incubator, cells were washed three times with PBS in order to remove any loosely attached or non-attached nanorods and then fixed in a 4% formaldehyde solution in PBS at room temperature for 10 min. The cells were then washed twice with PBS and incubated with 0.1% Triton X-100 (Sigma-Aldrich) plus 1% bovine serum albumin (BSA; Sigma-Aldrich) in PBS at room temperature for 15 min followed by 5 µg/ml 4',6-diamidino-2-phenylindole (DAPI; Molecular Probes) staining in PBS for 3 min at room temperature. The slides were washed twice with PBS, mounted with glycerol on the glass slide for microscopical observation.

Characterization

Transmission electron microscopy (TEM) was performed using a JEOL 2011 TEM operating at an accelerating voltage of 200 kV. Selected Area Electron Diffraction (SAED) was also observed from the regions of perpendicularly aligned CdS nanorods. UV-Vis spectroscopy and fluorescence measurements of the phase transferred solutions were carried on a Cary-300 Bio UV-Vis spectrophotometer operated at a resolution of 1 nm and a Varian Cary Eclipse Fluorescence Spectrophotometer respectively. X-ray photoelectron spectroscopy (XPS) measurement of the phase transferred nanorods was carried out in a Kratos Axis 165 spectrometer using monochromated Al Kα radiation (hυ= 1486.58 eV). High resolution spectra were taken for the following photoelectron transitions: Cd 3d, S 2p, O1s and C1s at a fixed analyser pass energy of 20 eV. The core level spectra were background corrected using the Shirley algorithm and the chemically distinct species were resolved using a mixed Gaussian-Lorentzian fitting

procedure. The core level binding energies (BE) were calibrated using C 1s at 284.8 eV. In order to decipher the plausible mechanism of the phase transfer process, a drop of the phase transferred CdS nanorods by F127 was observed on a clean glass slide under an optical microscope (Model:Axio Imager MAT, Carl Zeiss AG Light microscopy). Confocal microscopy was performed on "Carl-Zeiss Meta 710" instrument excited with a 405 nm laser. Scanning electron microscopy (SEM) of the phase transferred samples, drop-cast on a Si (111) substrate were performed by a Hitachi S-4800 machine. Localization of nanoparticles was performed using a spectral laser scanning microscope Meta 710 based on the Axio Observer II (Carl Ziess, Germany) equipped with a Zeiss Neofluor 20 x objective. Excitation wavelengths were 405 nm and 488 nm. All confocal images were acquired with the same settings with respect to laser intensity and detector gain. Optical sectioning was performed to obtain the pattern of spacial distribution nanorods (cell surface, intracellular compartments).

Results and discussion

The phase transfer of the nanorods was conducted by vigorous stirring of the nanorod-toluene solution with an aqueous solution containing pluronic copolymers. During this process, the transfer of CdS nanorods from the organic to the aqueous phase could be followed visually (Fig. 1A) where the bright yellow colour of the CdS nanorods in toluene was transferred to the aqueous layer containing 5ml of 3% F127. Aqueous solutions containing 3 % and 5 % F88 resulted in an incomplete transfer with the characteristic yellow colour present in both organic and the aqueous medium, Fig. 1B. A clear organic layer was only obtained when the concentration of F88 was raised to 20%, however the aqueous layer became extremely viscous, due to excess surfactants, and could not be separated, Fig. 1B. P123 was also found to be quite effective at phase transfer, achieving 100% phase transfer with a 3% surfactant concentration, Fig. 1C. However, in this case, CdS nanorods from the aqueous phase were found to form a separate layer when further diluted with water. Probably, P123 was able to drag the rods into aqueous layer but not able to provide an effective hydrophilic environment for solubilising in a polar solvent thoroughly. P65 was found to be least effective, regardless of percentage weight in solution, and a

vigorous stirring of organic and aqueous layer generated an emulsion inseparable (Fig. 1D) even after 3 days. Visual observation of the yellow colour from the aqueous part of F127 solution was in accord with the UV-Vis and photoluminescence spectra (Fig. 1E curves 1, 3) which shows characteristic features similar to CdS synthesised in the organic medium. The emission peak for F127 phase transferred CdS nanorods (curve 3 in Fig. 1E) centred at ~490 nm (band gap~ 2.53 eV) is almost 30 nm blue-shifted as compared to the emission spectra of bulk CdS (ca.510 nm). This is probably due to an enhanced quantum confinement within the nanorods. The presence of a satellite peak (~523 nm, green shifted) instead of a single sharp peak is possibly from the group of nanorods, a phenomenon which is generally observed when the nanorods are not isolated and are coupled to other nanocrystals. [24] The other broad absorption band ranging from 650-800 nm is generally attributed to the emission caused due to non-radiative decay of surface trap states of the semiconductor materials. In contrast, pristine F127 did not produce any emission in the visible region when excited at 350 nm (curve 2, Fig. 1E).

Fig. 1F shows the transmission electron micrograph of F127 protected CdS nanorod super crystals (NRSCs), ranging from 100-600 nm, that have resulted after a phase transfer to the aqueous medium. A higher magnification image, Fig. 1G, shows that each consists of an ensemble of axially aligned and close packed CdS nanorods. The inter-rod distance of the CdS phase transferred nanorods (Supporting information, Fig. S1b) was found to be ~3.5 nm. Interestingly, this is comparable to the interparticle distance obtained when the same nanorods are assembled on a substrate from an organic solution under Highly Oriented Pyrolytic Graphite as reported previously [12] (Supporting information, Fig. S1a). The absence of enhancement in the inter-rod spacing in the NRSCs when compared to rods assembled under HOPG strongly suggests that the rods are still tethered only by the long chain alkyl ligands in the close packed assembly. The triblock copolymer therefore does not interact individually with each alkyl capped rod but encloses a group or rods as an ensemble. Selected area electron diffraction (SAED) pattern obtained from F127 capped CdS nanorods, inset of Fig. 1G, is indexed to the reflections of wurtzite CdS (a, b=4.1409 A^0, c=6.7198 A^0, PCPDF File No: 41-1049). Similar results were obtained in the case of phase transfer of CdS nanorods by F88 where NRSCs ranging from 100-

400 nm was obtained with the individual rods being perpendicularly aligned within these structures. The UV-Vis and PL spectra along with representative TEM images of the F88 transferred CdS nanorods are shown in Supporting Information Fig. S2.

Phase transfer with CdSe nanorods and CdTe dipods/ tetrapods which were previously prepared through a similar pyrolytic route [4] having ODPA/OPA/HPA/TOPO as the surface capping agent were also studied. The phase transfer of monodisperse CdSe nanorods resulted in the formation of individual NRSCs ranging from 20-300 nm, Fig. 2A. A further magnified image, Fig. 2B, shows that NRSCs of similar size can further organise on a larger scale into a pseudo-hexagonal arrangement that mimics the close packing of individual rods within each super crystal (inset, Fig.2B). A high resolution image, Fig. 2C, of nanorods within an NRSC shows the lattice parameter (0.35 nm) from the highly oriented crystallographic planes (002) of the individual nanorods. The CdSe NRSCs were more monodisperse than equivalent CdS NRSCs and showed remarkably high water dispersibility requiring high centrifugation speeds for precipitation. Judicious size selection of the NRSCs was achieved by sequentially increasing the speed with the largest > 200 nm precipitating at 5500 rpm (Fig. 2D) and the smallest 20-80 nm at 13000 rpm (Fig. 2E). The smallest NRSCs which form a discernable disc from the axial alignment and close packing of nanorods were typically 40-50 nm in diameter, Fig. 2F.

TEM images (Fig. 2G-I) of phase transferred CdTe dipods/ tetrapods are somewhat different, though assembly can be found in some regions of the sample (Fig. 2G, H). The lack of NRSC formation tendency in tetrapods can be attributed to the fact that dipods/ tetrapods cannot be compressed easily like nanorods in the form of compact close packed structures. In spite of this fact, CdTe tetrapod-assembly are somewhat formed and transported to the aqueous phase which clearly establish the efficacy of F127 for phase transfer of semiconductor nanocrystals. To prove the crystalline nature of phase transferred CdSe and CdTe, SAED patters are given as inset in Fig. 2C and Fig. 2I respectively which correspond to the wurtzite structures (CdSe: a, b=4.299 A^0, c=7.010 A^0, PCPDF File No: 08-0459; CdTe: a, b=4.58 A^0, c=7.5 A^0, PCPDF File No: 19-0193).

X-ray photoelectron spectroscopy (XPS) of the CdS nanorods phase transferred by F127 and F88 was also performed. The C1s spectra in Fig. 3A and 3B clearly show the presence of 2 component peaks. The lower binding energy peak at 284.8 eV is assigned to carbon bonded to carbon or hydrogen. The appearance of a second component peak at 286.3 eV (deconvoluted curve 2 in Fig. 3A and B) can be assigned to C-O bonding present in both F127 and F88. The O1s spectra, Fig. 3C and 3D show the related Oxygen from the C-O bond appearing at 532.5 eV. The ratio of C: O for the C-O bonding is 2.1 and 1.9 for F127 and F88 transferred CdS nanorods respectively. This is in good agreement to the C: O ratio from the molecular formula of the ether linkages in F127 ($PEO_{106}PPO_{69}PEO_{106}$) and F88 ($PEO_{102}PPO_{39}PEO_{102}$). In contrast, C1s peak of only ODPA/TOPO capped CdS nanorods in the organic medium did not show any such high energy C1s peak corresponding to C-O (Supporting information, Fig. S3). The C-O containing species in the phase transferred samples constitute 50-60 % of the surface composition as determined by XPS. In addition, intensity of the alkyl peak (284.8 eV) corresponding to surfactant species decreases by half relative to that of CdS nanorods in the absence of the polymer, while the ratio of alkyl C: Cd of the nanorods remain comparable. This can be viewed as resulting from the screening effect imposed by the polymer, which supports the postulation that the polymer encapsulates the nanorods ensemble by interacting with the capping layer.

The proposition of encapsulation of a group of nanorods by F127 was further supported by scanning electron microscope (SEM) images. Discrete NRSCs could be resolved by SEM and at low resolution the structures appear as a mixture of spherical and anisotropic particles, Fig. 4A. HRSEM, Fig. 4B (scalebar= 100 nm) and further magnified in Fig. 4C (scalebar= 50 nm) revealed the individual nanorod close packing within the structures which forms a perfect hexagonal framework. The HRSEM image further confirms that all the NRSCs have a disc morphology predominantly consisting of a single monolayer of axially aligned rods. In the NRSC labelled 1 (Fig. 4B) the disc has come to rest flat on the substrate whereas in 2 the disc is on its edge. Some stray rods lie in a parallel orientation on the 2D assemblies but the predominant rod orientation is close packed within the disc. An estimate on a single NRSC as shown in the magnified image of Fig. 4C revealed that as many as ~800 nanorods are bound

together in this hexagonal closed-packed assembly. The occurrence of 2D assembly from nanorods in solution suggests a significant driving force for side by side packing of the rods. This effect parallels that observed from nanorods assembled on a substrate where supercrystallisation was evident with the nanorods finding their preferred place on the growing assembly before locking in thus allowing the lowest energy consideration to be reached. [11, 12, 15] Clearly, the similar formation of highly ordered nanorod discs from randomly dispersed nanorods in solution suggests a similar phenomenon is occurring on phase transfer. Particle size analysis, optical microscopy (Fig. S4a) and the ability to selectively precipitate by mass (centrifuge) or by size (filtration, Fig. S4b, c) confirmed that the NRSCs were real features present in solution and do not occur due to solvent evaporation.

Fig. 5 represents a schematic of the plausible mechanism where the phase transfer occurs by the aggregation and encapsulation of individual alkyl capped nanorods as a hydrophobic core most likely co-ordinated to a PPO corona and PEO shell of a triblock copolymer micelle. It is anticipated that there are *two factors* responsible for the phase transfer of CdS nanorods from toluene to water namely (1) hydrophobic-hydrophobic interaction between hydrophobic head groups of the copolymer and the long chain hydrocarbon of ODPA capping ligands on the CdS nanorods and (2) the hydrophilic tail of the copolymer should be sufficient to provide a good hydrophilic environment to the compact micelle like structure. Essentially it was seen that mere presence of a large hydrophobic head or a large hydrophilic tail is not sufficient for proper phase transfer. Among the set of four different triblock copolymer used in the experiment, F127 has the longest head and tail. So both the factors are applicable in this case, enabling a good protection to the hydrophobic core as well as providing a good hydrophilic environment, thus F127 worked best for the phase transfer. F88 has equivalent long hydrophilic tails like F127 but the head group is relatively smaller. Thus factor (1) is relatively weak and is not enough for an effective phase transfer. Therefore a lower concentration of F88 is not sufficient for 100% phase transfer, but on increasing the F88 concentration, the number of molecules interacting with CdS increases and as a result phase transfer capability was enhanced. The tail of the copolymer F88 was long and thus able to make the NRSC water dispersible without any difficulty. P123 has a long hydrophobic

head, so it can also successfully phase transfer CdS to water and satisfy factor (1), but short hydrophilic tail is responsible for its poor water dispersibility. For similar reasons phase transfer by P65 does not occur due to the combination of short head (PPO) as well as short tail (PEO).

Preliminary investigation of biological application was carried out by in-vitro analysis in a Human Vascular Smooth Muscle (VSM) cell-line which is a primary candidate for biomedical treatment for many cardiovascular pathologies. [25] Excitation (λ= 405 nm,) of the phase transferred CdS NRSCs by CLSM (Confocal Laser Scanning Microscope, Fig. 6A) yielded a characteristic fluorescence intensity in the blue and further confirmed the ease of dispersibility and homogeneous size distribution of the disc shaped assemblies (0.2- 0.6 μm range). The VSM cell-line was incubated with the NRSCs and their internalization, cellular uptake and intracellular distribution were further monitored. Uptake occurred without any transfection agents into the adherent VSM cell line and was efficient, fast and led to high loading into the cells, Fig. 6 B, E. Rapid and irreversible internalization starts during the first 20 minutes of incubation with no excretion or further aggregation even after 24 hours. With application of optical sectioning we were able to show two types of interaction between the cells and NRSCs: adsorption of the nanostructures on the cell membrane giving membranous fluorescence in the blue spectral region, Fig. 6C and internalization of the NRSCs inside the cell giving intracellular fluorescence in the red spectral region, Fig. 6D. Overall, there is a significant fluorescence intensity signal from NRSC treated cells (Fig. 6B-E) which allowed visualizing of all minor structural details of cell shape, cell surface morphology and adhesion to substrate. Strong fluorescence, cellular uptake and prolonged persistence in the human cells (up to 7 days in this study) make these ensembles potentially useful as fluorescent probes in a range of biological applications including for example flow cytometry techniques, cell–scaffold interaction studies and DNA markers. [26, 27] However, further details of the uptake mechanism, cytotoxicity, and photostability, will clearly need to be addressed. Water soluble NRSCs may have advantages over discrete nanorods in that the total intensity of emission is proportional to the number of rods and their size can potentially be tuned to specifically match different biological entities for example

a protein (5-50 nm) a virus (20-500 nm), or a gene (2 nm wide and 10-100 nm long). As an example, larger 300-400 nm NRSCs, while difficult to translocate to cell compartments, would still be small enough to transport in the blood vessel and capillary system.[28] NRSCs in the 100-300 nm range may have promising applications in imaging techniques of cardiovascular pathology, biosensors, liquid chromatography and bio separation methodology.[29-33] Since the NRSCs in this size range would be larger than the targeted species, they most likely would participate in binding without significant perturbation of the binding equilibrium and provide an efficient detection of a low amount of a target by microscopy or spectroscopical tools.[34, 35] Assemblies in the 30-100 nm range will be similar in size or smaller than the target species and may find use in applications such as FRET analysis,[36] hybridization or nanoscale analysis of low abundant proteins and peptides (nanoproteomics).[37]

Conclusion

In conclusion, we have demonstrated a facile route for the formation of water soluble NRSCs of CdS, CdSe and CdTe. The phase transfer occurs at room temperature with the encapsulation and close packing of a group of nanorods in the hydrophobic core of a triblock copolymer micelle. The method of transfer is generally applicable to any monodisperse solution of ligand capped nanorods. The order and axial alignment of the assemblies allows discrete nanorod properties such as fluorescence to be enhanced by collective emission. In this study, uptake of the water dispersible nanorod ensembles in a cell line showed strong membrane and cell specific fluorescence at low laser intensity. The range of sizes (50-600 nm) obtainable with water dispersible nanorod assemblies and the biocompatibility of their polymer shells have the potential to greatly extend both the range and diversity of biological applications possible with semiconductor nanocrystals.

Acknowledgment

13

Reference

1   J. Hu, L-S Li, W. Yang, L. Manna, L-W Wang, A. P Alivisatos, *Science*, 2001, **292**, 2060
2   S. A. Empedocles, R. Neuhauser, K. Shimizu, M. G. Bawendi, *Adv. Mater.*, 1999, **11**, 1243.
3   A. P. Alivisatos, *J. Phys. Chem.*, 1996, **100**, 13226.
4   I. Gur, N. A. Fromer, M. L. Geier, A. P. Alivisatos, *Science*, 2005, **310**, 462.
5   X. F. Duan, Y. Huang, R. Agarwal, C. M. Lieber, *Nature*, 2003, **421**, 241-245.
6   N.C. Greenham, X.G. Peng, A.P. Alivisatos, *Phys. Rev B.*, 1996, **54**, 17628.
7   J. S. Steckel, J. P.Zimmer, S.Coe-Sullivan, N. E Stott, V. Bulovic, M. G.Bawendi, *Angew. Chem. Int. Ed.*, 2004**, 43**, 2154.
8   S. Coe, W.K. Woo, M. Bawendi, V. Bulovic, *Nature*, 2002, **420**, 800.
9   R. Xie, D. Battaglia, X. Peng, *J. Am. Chem. Soc.*, 2007, **129**, 15432.
10 T. Zhai, X. Fang, Y. Bando, Q. Liao, X. Xu, H. Zeng, Y. Ma, J. Yao, D. Golberg, *ACS Nano*, 2009, **3**, 949.
11 K. M. Ryan, A. Mastroianni, K. A. Stancil, H. Liu, A. P. Alivisatos, *Nano Lett.*, 2006, **6**, 1479.
12 S. Ahmed, K. M. Ryan, *Nano Lett.*, 2007**, 7**, 2480.
13 C. O'Sullivan, S. Ahmed, Kevin M. Ryan, *J. Mater. Chem.*, 2008**, 18**, 5218.
14 C. C. Kang, C. W. Lai, H.C. Peng, J. J. Shyue, P. T. Chou, *ACS Nano*, 2008, **2**, 750.
15 Y. Min, M. Akbulut, K. Kristiansen, Y. Golan, J. Israelachvili, *Nat. Mater.*, 2008, **7***, 527.
16 J.K Jaiswal, H. Mattoussi, M. J. Mauro, S. M. Simon, *Nat. Biotech.*, 2003**, 21**, 47.
17 W. J. Parak, D. Gerion, T. Pellegrino, D. Zanchet, C. Micheel, S. C. Williams, R. Boudreau, M. A. L. Gros, C. A. Larabell, A. P. Alivisatos, *Nanotechnology*, 2003, **14**, R15-R27.
18 L.-S. Li, J. Walda, L. Manna, A. P. Alivisatos, *Nano Lett.*, 2002, **2**, 557.
19 Z. Nie, *et al. Nat. Mater.*, 2007**, 6**, 609.
20 J. Zhuang, Andrew D. Shaller, J. Lynch, H. Wu, Ou. Chen, Alexander D. Q. Li; Charles Y. Cao, *J. Am. Chem. Soc.*, 2009, **131**, 6084.
21 K. M. Ryan, N. R. B. Coleman, D. M. Lyons, J. P. Hanrahan, T. R. Spalding, M. A. Morris, D. C. Steytler, , R. K. Heenan, , J. D. Holmes, *Langmuir*, 2002**, 18**, 4996.
22 A. V. Kabanov, E. V. Batrakova, V. Y. Alakhov, *J. Control.Release*, 2002, **82**, 189.
23 H. Liu, J. S. Owen, A. P. Alivisatos, *J. Am. Chem. Soc.*, 2007, **129**, 305.
24 H. Htoon, J. A. Hollingworth, A. V. Malko, R. Dickerson, V. I. Klimov, *Appl. Phys. Lett.*, 2003, **82**, 4776.
25 U. Westedt, L. Barbu-Tudoran, A.K. Schaper, M. Kalinowski, H. Alfke, T. Kissel, *AAPS PharmSci.*, 2002**, 4,** 206.
26 Bulte, J. W.M.; Modo M. M. J. (Eds.*) Nanoparticles in Biomedical Imaging Emerging Technologies and Applications In Fundamental Biomedical Technologies*, ed. by J. W.M Bulte, M. M.J. Modo, New York, USA 2008, Vol.3, XVIII.
27 A. Merkoci, *FEBS Journal*, 2006**, 274**, 310.
28 F. Gentile, M. Ferrari, P. Decuzzi. *Ann Biomed Eng.*, 2008, **36**, 254.
29 *Biofunctionalization of Fluorescent Nanoparticles. Nanotechnology in Biology and Medicine –Methods, Device and Application -Methods, Devices, and Applications*, 2006. Taylor & Francis Group, LLC.
30 J. L. Swift , D.T. Cramb, *Biophysical Journal*, 2008**, 95**, 865.
31 D. P. Kalogianni, T. Koraki, T. K. Christopoulos, P. C. Ioannou, *Biosens Bioelectron.*, 2006, **21**, 1069.

32 W.-J. Chen, P.-J. Tsai, Y.-C. Chen, *Anal. Chem.*, 2009, **81**, 1722.
33 H. M. E. Azzazy, M. M. H. Mansour, S. C. Kazmierczak*, Clin. Chem.*, 2006**, 52**, 1238.
34 M. Brehm, T. Taubner, R. Hillenbrand, F. Keilmann, *Nano Lett.*, 2006, **6**, 1307.
35 M. Breunig, S. Bauer, A. Goepferich. *Eur J Pharm Biopharm.*, 2008, **68**, 112.
36 W. Jiang, B.Y.S. Kim. J.T. Rutka, W.C.W. Chan, *Nat. Nanotech.*, 2008**, 3**, 145.
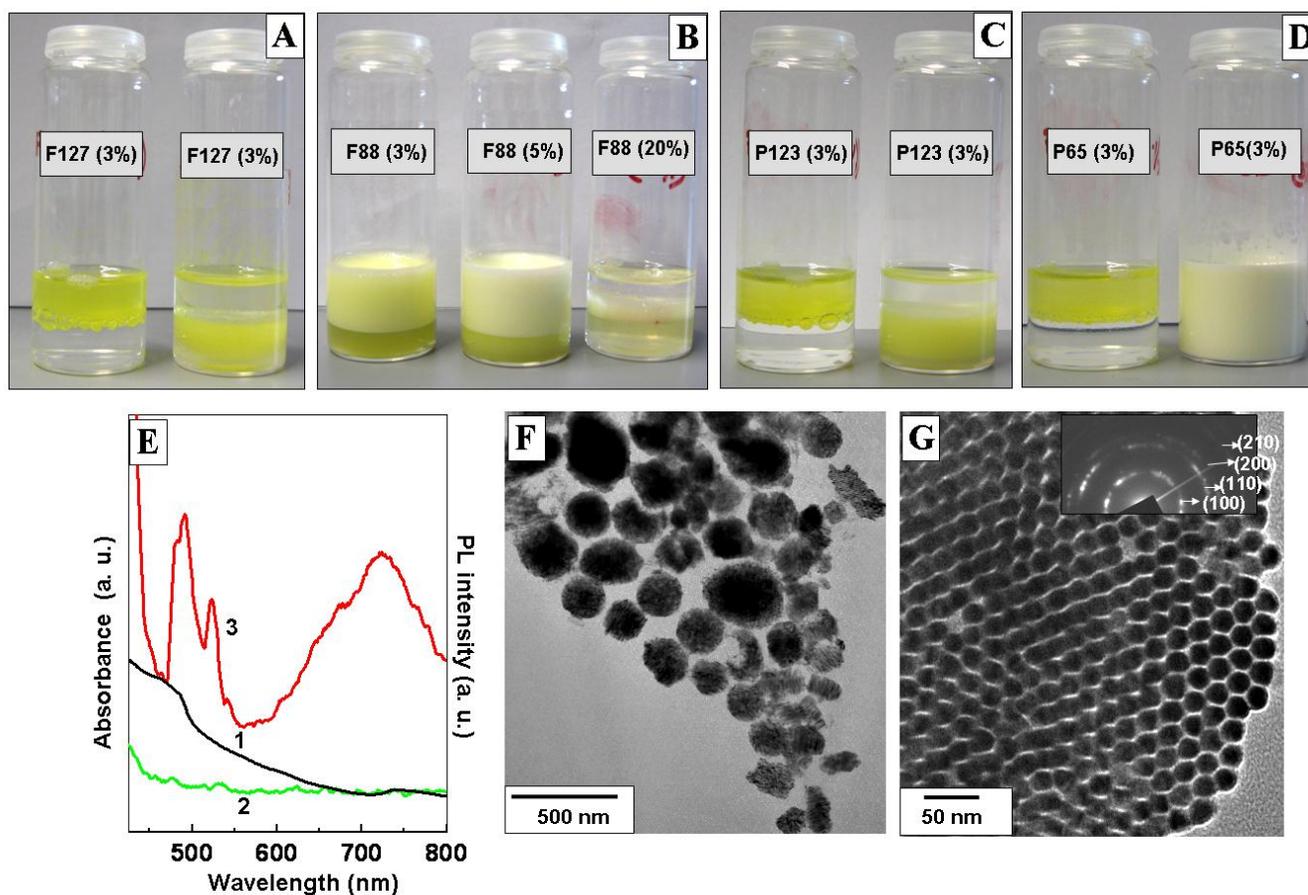37 D. A. Egas, Mary J. Wirth, *Annu. Rev. Anal. Chem.*, 2008, **1***, 833.

Fig. 1 Macroscopic, optical and electronic characterization of phase transferred CdS nanorods. (A) Photographs of sample vials showing the phase transfer of CdS nanorods from toluene with 3% F127, (B) 3%, 5% and 20% F88, (C) 3% P123 and (D) 3% P65 into water. In the Fig.s (A), (C) and (D) CdS nanorods are in toluene in the bottle on the left-hand side (upper layer), whereas they are transferred to the aqueous phase (bottom layer) in the right-hand side bottle. (E) UV-Vis and photoluminescence spectra of CdS nanorods phase transferred with F127 (curves 1 and 3 respectively) in the aqueous phase. Curve 2 is the emission spectra of pristine F127. (F) Representative TEM images of the phase transferred CdS nanorods in water by F127 revealing NRSCs and (G) Perpendicular alignment of the nanorods magnified from one of the assemblies shown in F. The inset in (G) shows the selected area electron diffraction (SAED) pattern taken from the corresponding assembly of CdS nanorods.
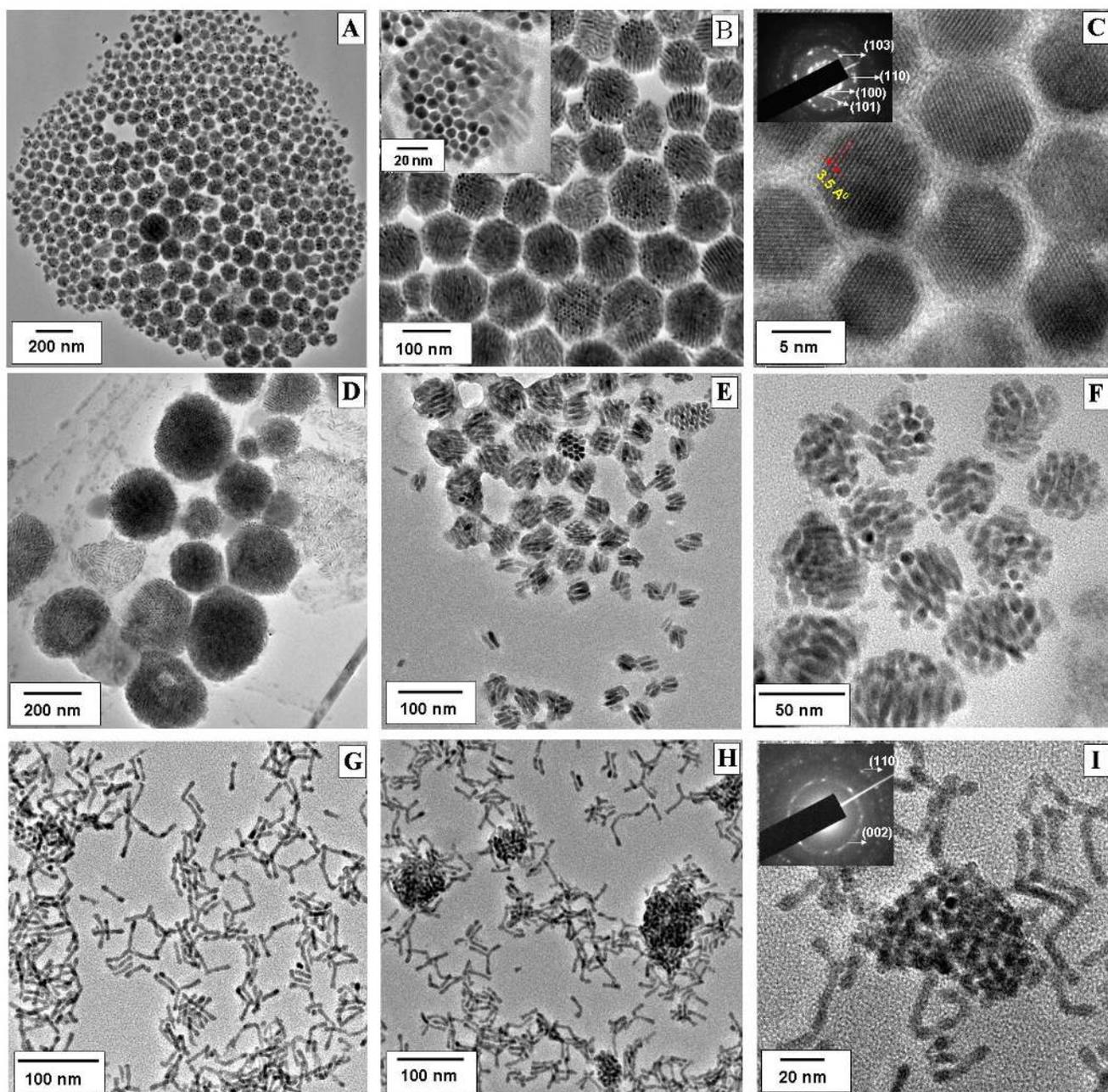
Fig. 2 Electron microscopy characterization of CdSe and CdTe samples (A) Representative TEM image of the formation of F127 mediated CdSe nanorod assemblies extending from 20-300 nm. Closed packed pseudo-hexagonal assembly of the nanorods is revealed in (B) and its corresponding inset shows the hexagonal stacking of the individual nanorods inside the micelle like structure. (C) High resolution TEM image of the individual nanorods within the NRSCs showing the crystallographic planes with the corresponding SAED pattern shown in the inset. Step-wise size selective centrifugation of NRSCs resulting in the larger (>200 nm, TEM image of D) and consequently smaller assemblies (20-80 nm, TEM image of E). Fig. F shows the TEM image of the smallest disc (40-50 nm) resulted from the alignment and packing of the individual nanorods. (G) Representative TEM image of the phase transferred CdTe dipods/ tetrapods. (H) and (I) are TEM image snapshots of the CdTe solution showing formation of few assemblies as compared to that of CdSe. SAED pattern (inset of I) confirm the crystalline nature of the phase transferred CdTe NRSCs.
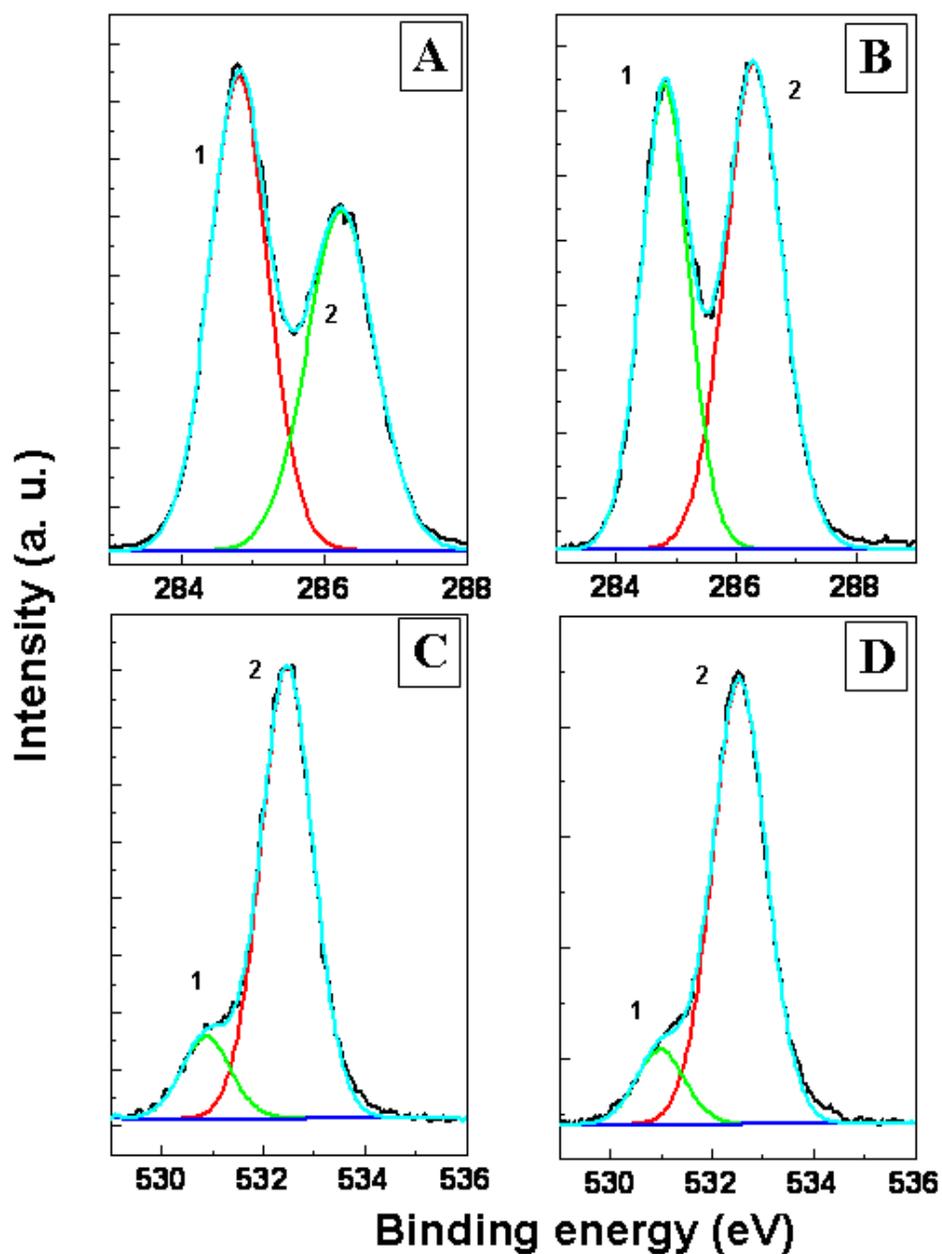
Fig. 3 C1s and O1s core level spectra recorded from a drop-cast film on a glass substrate from the CdS nanorods in aqueous phase that have been phase transferred with F127 (A) and (C) and with F88 (B) and (D) respectively. The chemically distinct deconvoluted components have been shown as curves 1 and 2 in all the Fig.s.
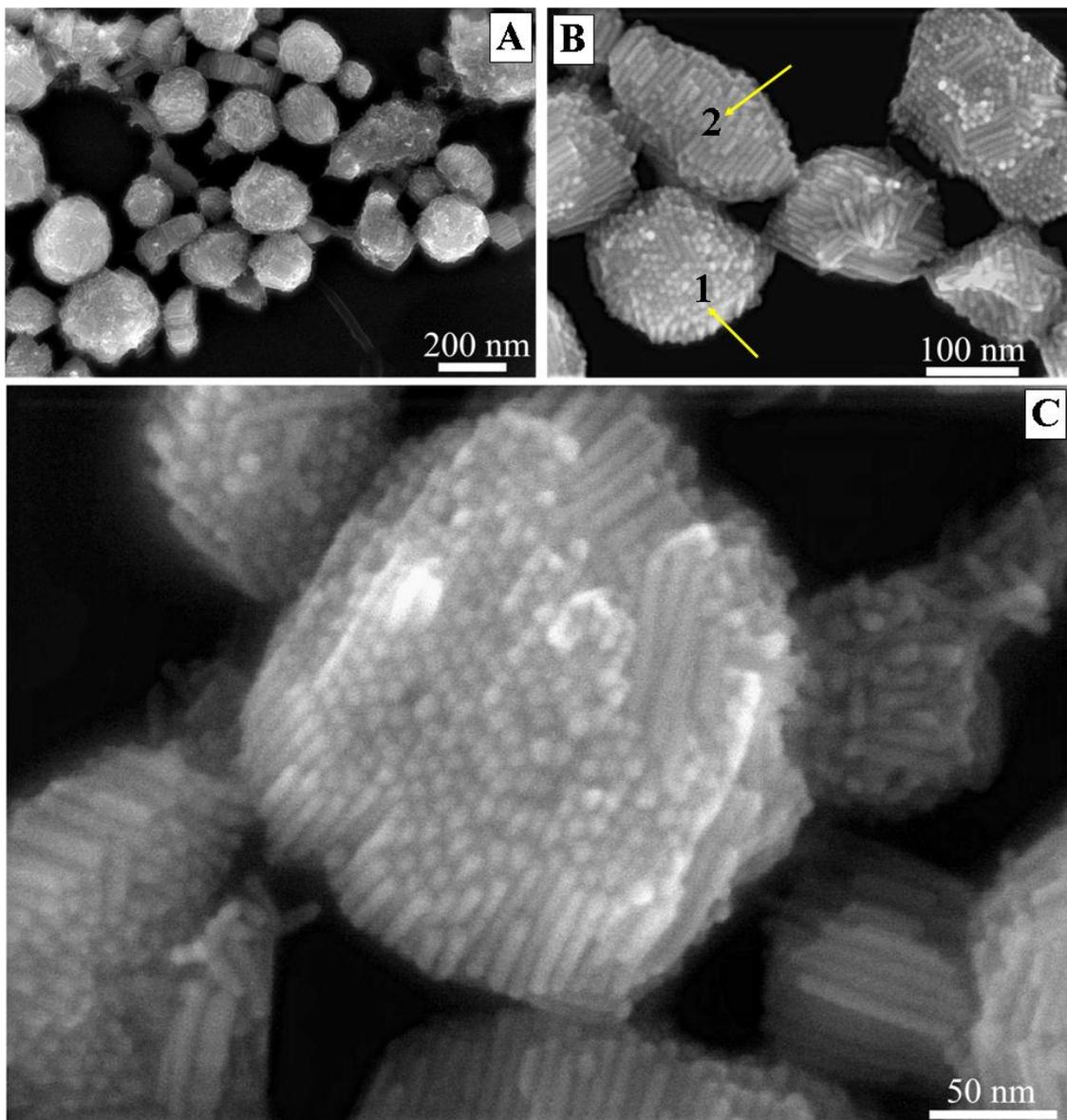
Fig. 4 SEM, HRSEM of the NRSCs. (A) shows the SEM image CdS nanorods phase transferred by F127 in the aqueous phase showing different sized anisotropic nanorods assemblies. (B) HRSEM image where one of the NRSCs are lying flat (point 1) or are on its edge (point 2). (C) Further magnified image of one of the NRSCs revealing the multiple number of individual CdS nanorods stacked into a single structure.
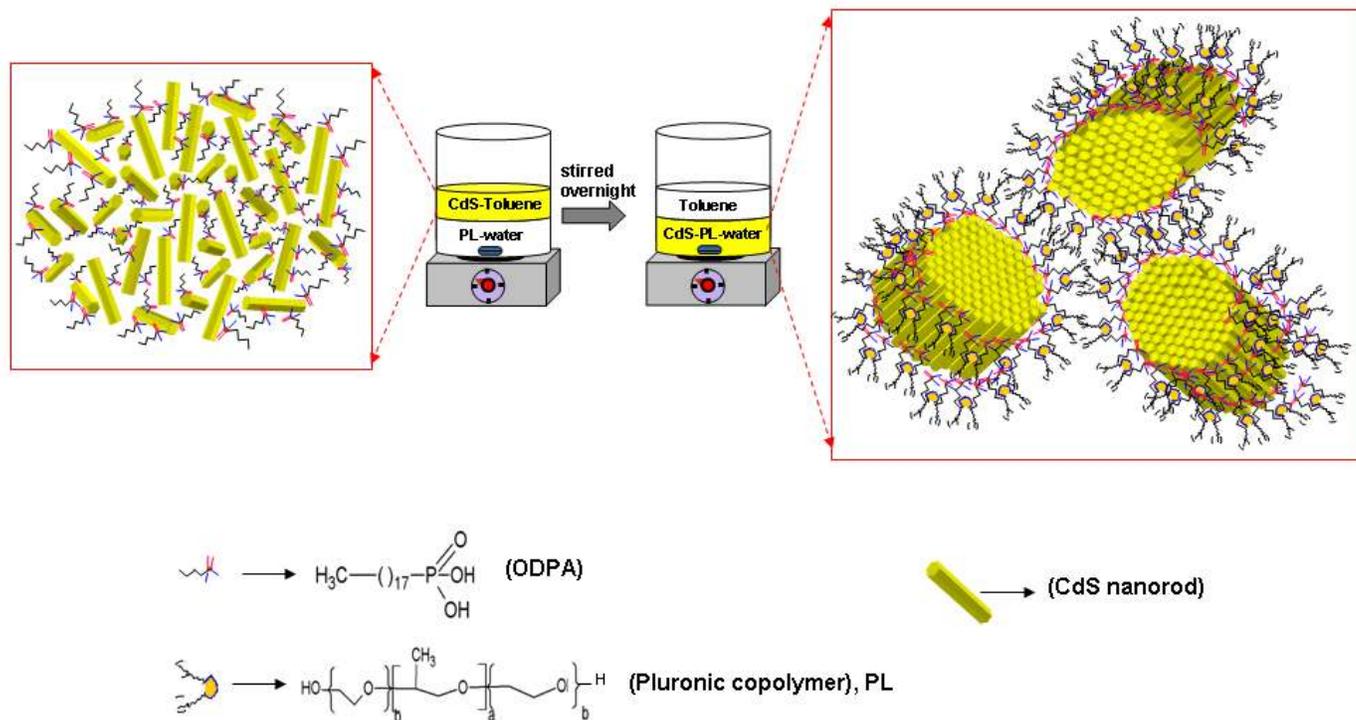
Fig. 5 Proposed reaction mechanism pathway. Schematic showing the 3D orientation of the CdS nanorods in toluene and after reverse phase transfer to the aqueous phase with the help of copolymers via a micelle-type of structure.
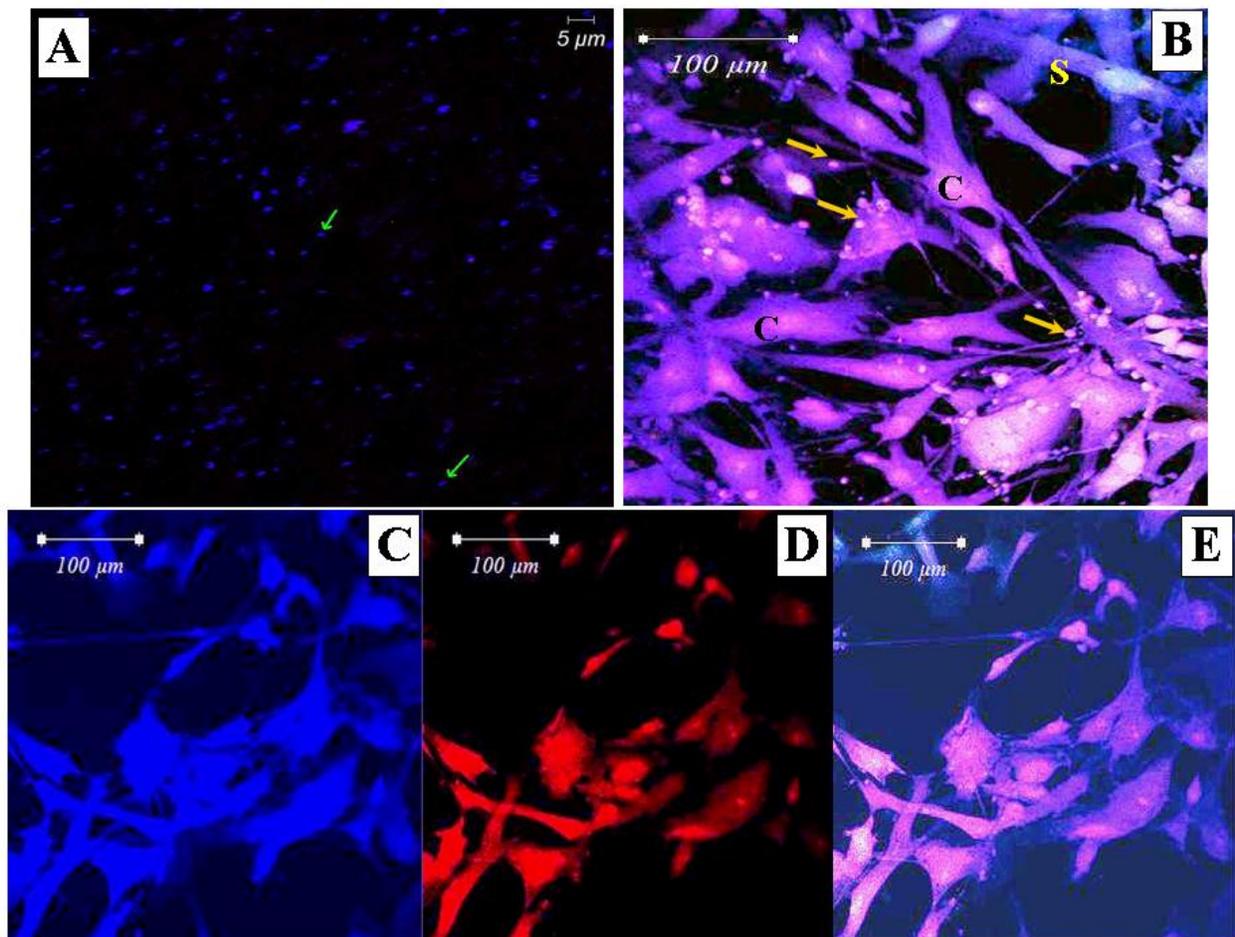
Fig. 6 Preliminary investigation of cellular biocompatibility of CdS assemblies, cellular uptake and maintainance of the fluorescent properties after internalisation into cytosol. (A) LSCM image of phase transferred CdS NRSCs. (Excitation laser λ=405 nm. Emission detection were collected in the range λ = 420-480 nm), (B) Cellular uptake of CdS nanorods by VSM cells. LSCM images of CdS NRSCs adsorbed onto VSM cell outer membrane after 3 h incubation and internalisation of CdS NRSCs into the cell cytoplasm of VSMC cell via endocytosis can be observed on the cell surface membrane. After internalisation spectral properties of the NRSCs are shifted to red spectra. Arrows shows the location of event of CdS uptake by the cells, (C) LSCM image of CdS NRSCs localised onto VSMC cell outer membrane after 24 h incubation and they are shown to produce only a fluorescence signal in the blue spectral region (Excitation laser λ=405 nm. Emission detection were collected in the range λ = 420-480 nm), (D) Internalised CdS NRSCs into the cell cytoplasm of VSMC cell are shown to have an emission in the red spectral region λ=660-690 nm, (E) Total fluorescent signal from the CdS nanorods treated cell shown on a merged image of the two spectral detection channels.

Graphical Illustration
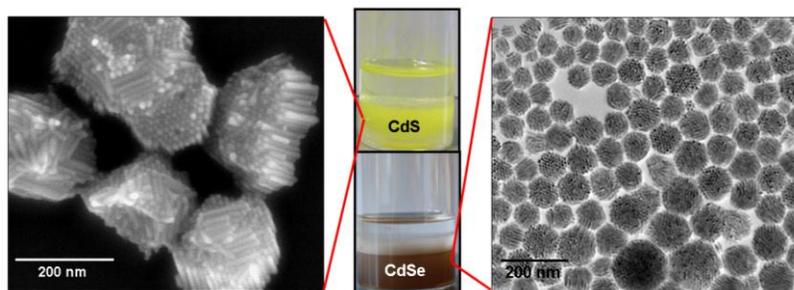
Phase transfer of CdS, CdSe nanorods dispersed in toluene into aqueous medium by pluronic block copolymers has resulted in the formation of 2D disk shaped assemblies which showed strong membrane and cell specific fluorescence at low laser intensity.